International Journal of Thermophysics, Vol. 25, No. 3, May 2004 (© 2004)

Phase Behaviors of Binary Hard-Sphere Mixtures Using Simple Analytical Equations of State

A. Yokozeki[1]

Received June 18, 2003

Recently, we have proposed a unified analytical equation of state (EOS) for solid–liquid–vapor states of matter, and have examined the thermodynamic properties of argon, carbon dioxide, and methane, as well as binary mixtures of methane and carbon dioxide. Also it has been demonstrated that the EOS can be applied for the solid–fluid transition of hard spheres, by eliminating the attractive part of the EOS. The present work is an extension of the earlier calculations for identical hard spheres, and here we examine the phase behavior of binary hard-sphere mixtures. The hard-sphere EOS employed in this study is

$$P = \frac{RT}{V-b}\left(\frac{V-d}{V-c}\right)^k,$$

where $k=1$ or 2, and $k=0$ [or $c=d=0$] as a special case. b, c, and d are proportional to a hard-sphere volume, and their mixing rule is a quadratic form in mole fraction x, with a mixing parameter l_{ij} ($l_{ij}=l_{ji}$ and $l_{ii}=0$). The b parameter is given by

$$b = \sum_{i,j=1}^{2} \frac{(b_i+b_j)}{2}\left(1-l_{ij}\right)x_i x_j.$$

Similar mixing rules are applied to c and d. It is shown that various fundamental phase-transition behaviors can be described: ideal or near ideal, azeotropic (maximum and minimum), eutectic, eutectoid, monotectic, peritectic types, and stable fluid–fluid de-mixings without becoming metastable due to the interference of solid–liquid phase transitions. Rather complicated phase diagrams with a combination of various types are also predicted. The present

[1] DuPont Fluoroproducts Laboratory, Chestnut Run Plaza 711, Wilmington, Delaware 19880, U.S.A. E-mail: akimichi.yokozeki@usa.dupont.com

0195-928X/04/0500-0643/0

study is a starting point and is useful for understanding the global topology of solid–liquid–vapor phase transitions of binary mixtures.

KEY WORDS: equation of state; hard spheres; liquid; mixtures; phase diagrams; solid; thermodynamics.

1. INTRODUCTION

Perhaps the hard-sphere model and the Ising model are the most important tools in the field of statistical physics and thermodynamics. Although it is merely a model with the hard-core repulsive potential, often it provides a good description of thermodynamic behaviors for actual compounds, particularly for condensed-phase properties, where the excluded volume (geometrical) effect is a dominant factor. Also it acts as a starting point in perturbation theories for modeling actual substances. Therefore, numerous studies of hard-sphere systems have been reported in the past and no doubt will continue in the future. A brief history of such studies is given in a recent article [1], and also any standard textbook for statistical physics describes this important model (for example, Ref. 2).

One of the most exciting accomplishments may be that the equation of state (EOS) for hard-sphere ensembles was analytically solved based on the Percus–Yevick approximation of the exact integral equation in the theory of fluids [3], although the EOS resulted in two different equations ("pressure" and "compressibility" equations). This thermodynamic inconsistency having two different EOS forms is due to the assumptions used. The fluid properties of hard spheres by the EOS are in a good agreement with those of computer simulations or by the virial expansion EOS [2]. However, the derived EOS does not show any phase transition (or singularity) within the physically meaningful region. On the other hand, other approximations, such as the Kirkwood equation or Yvon–Born–Green equation, cannot be solved analytically. But, by numerical analysis, Kirkwood and Boggs [4] predicted an instability of the fluid state, well below the closest packing density of a solid, indicating a possible fluid–solid phase transition for hard spheres. Such a phase transition with the purely repulsive interaction was indeed conceptionally curious but a quite fascinating phenomenon if it were real. This is because of the well-known fact that phase transitions like familiar vapor–liquid equilibria occur when two opposing (repulsive and attractive) factors are operating in the system.

Later, Alder and Wainwright [5] and Wood and Jacobson [6] confirmed such a phase transition independently by computer simulation using molecular dynamics and Monte Carlo methods. The physical meaning of the transition is still debatable. Some argue that it is due to the

purely entropic effect (an increase in the entropy of particles inside the solid "cells" with respect to the fluid state) [1]. However, the present author prefers the concept of the "statistical (kinetic) attraction" effect of the purely repulsive force at high density [2]. Or in terms of the language of statistical mechanics, it may be argued that some geometrical exclusion (contribution of small "watermelons") in the cluster integrals neglected in the Percus–Yevick approximation is responsible for such a phase transition [2, 7].

The study of mixtures of hard spheres and/or hard non-spherical bodies is a natural extension of the pure hard-sphere model and has been an active research field in recent years [8–15]. In the last decade, it was found that binary hard-sphere mixtures show extremely rich phase behavior [1]. Hard-sphere and hard-body mixtures are also important starting models for actual colloid–polymer mixtures or liquid-crystal solutions [16, 17]. The theoretical approaches for these mixtures are either integral equation theories or virial expansions of the mixture equation of state. Although both theoretical methods are well established, results are notoriously sensitive to the details of the approximations, and the existence or non-existence as well as the location of the phase transition is particularly susceptible. The fluid–solid phase boundary is also very sensitive to the choice of assumptions [1]. On the other hand, direct computer simulations may seem straightforward, and many interesting results have been reported using various inter-particle potentials [18, 19]. However, besides a large amount of computational time, results are not always reliable due to sluggish numerical convergence or very slow equilibration for highly asymmetric (size) mixtures [1, 8]. Many theoretical studies have been devoted to the virial expansion equation, where no solid state exists, and the phase transition, if it occurs, means fluid–fluid separation (de-mixing). One of the interesting questions is whether fluid–fluid de-mixing occurs in hard-sphere mixtures with the purely repulsive interaction. This is still debated. Even if it is predicted, it is not certain whether such a phase transition is thermodynamically stable with respect to the interference of solid–fluid phase transitions, as discussed in a recent article [8]. In their brief review of hard-sphere mixtures, Dijkstra et al. [1] stated in summary, "The predicted phase behavior of binary hard-sphere mixtures is very sensitive to the details of the theoretical approaches, and the character of the fluid–fluid and fluid–solid transitions and their interplay remains poorly understood."

Apart from numerous fundamental and theoretical studies mentioned above, to our knowledge, there is no report on hard-sphere mixtures based on empirical or engineering approaches. This may be due to the fact that many existing empirical, practical equations and methods are intended to

deal with actual substances, not for purely model compounds such as hard spheres. Furthermore, these equations are applied only for the fluid state, and in order to include the solid state, separate and/or different equations must be employed. The solid–fluid phase transition characteristics of real compounds play important roles in the field of practical and industrial applications. Phase diagrams of alloys in metallurgical applications are good examples, where regular (or quasi-regular) solution models are often successfully used to describe the solid–liquid phase diagrams [20]. Although the existing models and methods may be sufficient for practical and engineering applications to explain and/or correlate the observed solid–liquid phase-transition behavior, they should also be able to say something about the limiting case, i.e., (purely repulsive) hard spheres, at least qualitatively. Analytical simple EOS are far more convenient and useful to construct complicated solid–fluid phase diagrams of mixtures. In order to understand the global phase-transition behavior of binary hard-sphere mixtures, such EOS will be highly desirable and may provide important insights and information on the sensitive theoretical assumptions mentioned earlier.

Recently we have proposed an analytical unified EOS for solid, liquid, and vapor phases [21]. It can be written in a general form as

$$P = \frac{RT}{V-b}\left(\frac{V-d}{V-c}\right)^k - \frac{a}{V^2+qbV+rb^2}. \tag{1}$$

This may be regarded as an extension of the van der Waals (fluid only) EOS. Without the 2nd term (attractive term), it represents an EOS for hard spheres. In fact, the well-known solid–liquid phase transition of identical hard spheres was described well with this EOS [21]. The purpose of the present work is to analyze hard-sphere mixtures and to see whether this simple analytical EOS is capable of describing various solid–liquid phase transition characteristics. Furthermore, this study will be a starting point to understand the global topological classification of solid–liquid–vapor phase behaviors of binary mixtures [19, 22, 23]. It should be remembered that the well-known global topological classification (five out of six classes) for liquid–vapor phase diagrams of binary mixtures was made using a simple and empirical van der Waals EOS [24].

The organization of the present paper is as follows. Section 2 describes the hard-sphere EOS, which is the case of $a = 0$ of Eq. (1). The mixing rules and physical meanings of the constants b, c, and d are discussed, and the fugacity coefficients for three EOS forms with the exponent k of 0, 1, and 2 are derived. In Section 3, we discuss the analyses and results of phase diagrams for binary hard-sphere mixtures. First, a special case of $k=$

0 (or $c=d$), which becomes simply the repulsive part of the van der Waals EOS, is examined. Although it only presents purely fluid (or purely solid) states, the analysis provides good physical insights on the mixing parameters used in the present study. In addition, it is shown that the well-known regular solution model [20, 25] can be derived from this simple form of EOS: this proof is given for the first time, to the author's best knowledge. Next, various phase diagrams are presented using EOS with $k=1$ and $k=2$. Section 4 gives some discussions of the present results and related subjects, and then concluding remarks follow.

2. EQUATIONS OF STATE

By eliminating the attractive term ($a=0$) of Eq. (1), a hard-sphere EOS becomes

$$P=\frac{RT}{V-b}\left(\frac{V-d}{V-c}\right)^k=\frac{RT}{V-b}\left(1+\frac{c-d}{V-c}\right)^k, \tag{2}$$

and the compressibility factor Z is given by

$$Z=\frac{V}{V-b}\left(\frac{V-d}{V-c}\right)^k, \tag{3}$$

where b, c, and d for pure hard spheres are proportional to the hard-sphere volume, k is zero or a positive integer, and R is the universal gas constant. The form of the second equal sign in Eq. (2) provides a physical meaning of this EOS. The term $(c-d)/(V-c)$ is a correction to the van der Waals' repulsive term. Since the valid EOS form satisfies the condition, $V>b$ and $b<d<c$, as discussed in Ref. 21, this correction term becomes negative for a region $b<V<c$, where the solid state resides. The negative sign means the correction is *attractive*. This effective attraction reflects the so-called "kinetic attraction" force in a high-density state of hard spheres [2]. This interpretation suggests the existence of a similar but another type of hard-sphere EOS, which will be discussed briefly in a later section. Thus, there are some theoretical justifications for the present model, although it is a purely empirical and phenomenological EOS.

N-component mixtures [$N=2$ for the present study] are modeled by the following quadratic mixing rule with each pure component parameter and binary interaction parameters, l_{ij}, m_{ij}, and n_{ij}, where $l_{ij}=l_{ji}$ and $l_{ii}=$

0, and similar relations hold for m_{ij} and n_{ij}. Such mixing rules are often used in the van der Waals type EOS

$$b = \sum_{i,j=1}^{N} \frac{(b_i + b_j)}{2} \left(1 - l_{ij}\right) x_i x_j = b_1 x_1 + b_2 x_2 - l_{12}(b_1 + b_2) x_1 x_2, \tag{4}$$

$$c = \sum_{i,j=1}^{N} \frac{(c_i + c_j)}{2} \left(1 - m_{ij}\right) x_i x_j = c_1 x_1 + c_2 x_2 - m_{12}(c_1 + c_2) x_1 x_2, \tag{5}$$

$$d = \sum_{i,j=1}^{N} \frac{(d_i + d_j)}{2} \left(1 - n_{ij}\right) x_i x_j = d_1 x_1 + d_2 x_2 - n_{12}(d_1 + d_2) x_1 x_2. \tag{6}$$

Although the interaction parameter is introduced here as an empirical adjustable parameter, it has a physical meaning as discussed below. The non-zero parameter l_{ij} (or m_{ij}, n_{ij}) may be physically necessary when quadratic mixing in mole fraction is applied. The quadratic mixing is based on theoretical work [26] of the virial expansion equation for mixtures, where a random mixing assumption is employed. However, random mixing is valid only for molecules (or particles) with the same (or similar) sizes, or for sufficiently low densities of mixtures. When the size is very different and the density becomes sufficiently high (condensed phase), the cross term, $b_{ij} x_i x_j (i \neq j)$, cannot be symmetric with respect to the mole fraction, due to the geometrical restriction of the nearest neighbors. For example, the coordination numbers for a small particle (i) surrounded by large particles (j) and a large particle (j) surrounded by small particles (i) are different. Therefore, the inter-particle collision probability will not simply be a symmetric $x_i x_j$ factor [27] and can be highly complex. A similar discussion in this regard is given in Ref. 28. Concerning the effect of size differences, often volume fractions instead of mole fractions are used in mixing equations such as Eqs. (4)–(6), because they allow for the effect of size differences upon mixing in a more nearly adequate way than do mole fractions [25]. With a volume fraction φ_i, the parameter b without an empirical binary interaction parameter is given by

$$b = \sum_{i,j=1}^{2} \frac{(b_i + b_j)}{2} \varphi_i \varphi_j = b_1 \varphi_1 + b_2 \varphi_2, \tag{7}$$

where

$$\varphi_i = \frac{b_i x_i}{b_1 x_1 + b_2 x_2}. \tag{8}$$

In terms of mole fractions, Eq. (7) can be rearranged as

$$b=\frac{b_1^2x_1}{b_1x_1+b_1x_2}+\frac{b_2^2x_2}{b_1x_1+b_1x_2}=b_1x_1+b_1x_2+\frac{(b_1-b_2)^2}{b_1x_1+b_1x_2}x_1x_2. \tag{9}$$

By comparing this equation with Eq. (4), l_{ij} is equated to

$$l_{12}=l_{21}=-\frac{(b_1-b_2)^2}{(b_1+b_2)\,(b_1x_1+b_2x_2)}. \tag{10}$$

In this case, l_{ij} becomes a function of mole fractions, and then the mixing becomes non-quadratic in mole fractions. If the size difference is not too large, it may be appropriate to take an average of $b_1x_1+b_2x_2$ as $(b_1+b_2)/2$. Then Eq. (10) becomes

$$l_{12}=l_{21}=-2\left(\frac{b_1-b_2}{b_1+b_2}\right)^2 \tag{11}$$

Thus, the physical meaning of l_{ij} (or m_{ij}, n_{ij}) may be an effective average correction when the quadratic mixing in mole fractions is applied and when the size difference is not too large. Naturally, l_{ij} (or m_{ij}, n_{ij}) the size difference. It is useful to obtain such a relationship, since it will provide a further insight into the physical meaning of these binary interaction parameters.

Take the parameter b for example. Within the van der Waals theory, it represents the excluded volume of a pair of hard spheres times Avogadro's number (N_A). The per particle excluded volume of identical hard spheres (diameters in σ_i) is given by

$$b_{ii}\equiv b_i=\frac{4\pi}{3}\left(\frac{\sigma_i+\sigma_i}{2}\right)^3\frac{1}{2}=\frac{2\pi}{3}\sigma_i^3. \tag{12}$$

The factor 1/2 in this equation arises from excluding the double counting of the same particle. For non-identical hard spheres, a similar excluded volume exists, but a slight modification is required in order to take into account a possible non-additive effect on the collision diameter,

$$b_{ij}=\frac{4\pi}{3}\left(\frac{\sigma_i+\sigma_j}{2}(1+\alpha)\right)^3\frac{1}{2}=\frac{2\pi}{3}\left(\frac{\sigma_i+\sigma_j}{2}\right)^3\beta,\quad \beta\equiv(1+\alpha)^3. \tag{13}$$

The parameter α (or β) is an empirical correction to "additive hard spheres" (or "non-additive" correction), although the physical meaning is not obvious. Then, using Eqs. (12) and (13) while taking into account

Avogadro's number, the total excluded volume b on a molar basis can be expanded as

$$b = \sum_{i,j=1}^{2} b_{ij} x_i x_j = b_1 x_1 \left\{ x_1 + \frac{\beta}{4} (1+3\gamma)\, x_2 \right\} + b_2 x_2 \left\{ x_2 + \frac{\beta}{4} \left(1 + \frac{3}{\gamma} \right) x_1 \right\}, \tag{14}$$

where

$$\gamma \equiv \sigma_2/\sigma_1 = (b_2/b_1)^{1/3}. \tag{15}$$

After some algebraic manipulations and use of $x_1 + x_2 = 1$, Eq. (14) is rearranged as

$$b = b_1 x_1 + b_2 x_2 - \frac{3}{4} \left\{ \frac{(1-\gamma)^2}{1-\gamma+\gamma^2} - \frac{\beta-1}{3} \right\} (b_1 + b_2)\, x_1 x_2. \tag{16}$$

By comparing this with Eq. (4), we can identify the empirically introduced parameter l_{12} as

$$l_{12} = l_{21} = \frac{3}{4} \left\{ \frac{(1-\gamma)^2}{1-\gamma+\gamma^2} - \frac{\beta-1}{3} \right\}. \tag{17}$$

It is a function of the size ratio of hard spheres (γ) and the "non-additive" parameter (β). Thus, like l_{12} itself, the physical meaning of α(or β) can be regarded as an effective average correction for mixing when the quadratic mixing (or random mixing) is applied.

When we discuss the phase behavior with EOS, the fugacity coefficient is needed for the equilibrium calculation. The fugacity coefficient of the ith component, ϕ_i, is calculated from the following standard thermodynamic relation with a total number of moles, n, and the ith component mole number n_i [29],

$$\ln \phi_i = \int_V^\infty \left[\left(\frac{\partial n Z}{\partial n_i} \right)_{T,nV,n_j} - 1 \right] \frac{dV}{V} - \ln Z \tag{18}$$

In the case of EOS with $k = 1$

$$\ln \phi_i = \frac{1}{(b-c)^2} \left[(d-c)\, b_i' + (b-d)\, c_i' + (b-c) \left(d - d_i' \right) \right] \times \ln \left| \frac{V-b}{V-c} \right| - \frac{c}{b-c} \ln \left| \frac{V-c}{V-b} \right| - \ln \left| \frac{V-d}{V-c} \right|$$

$$+\frac{1}{b-c}\left[\frac{(d-b)\,b_i'}{V-b}+\frac{(c-d)\,c_i'}{V-c}\right], \tag{19}$$

where b_i', c_i', and d_i' for N-component mixtures and for N=2 are defined as

$$b_i' \equiv b-2\sum_{j=1}^{N}\frac{(b_i+b_j)}{2}\left(1-l_{ij}\right)x_j=-b_i+l_{12}\,(b_1+b_2)\,(1-x_i)^2\,, \tag{20}$$

$$c_i' \equiv c-2\sum_{j=1}^{N}\frac{(c_i+c_j)}{2}\left(1-m_{ij}\right)x_j=-c_i+m_{12}\,(c_1+c_2)\,(1-x_i)^2\,, \tag{21}$$

$$d_i' \equiv d-2\sum_{j=1}^{N}\frac{(d_i+d_j)}{2}\left(1-n_{ij}\right)x_j=-d_i+n_{12}\,(d_1+d_2)\,(1-x_i)^2\,. \tag{22}$$

In the case of EOS with $k=2$,

$$\begin{aligned}\ln\phi_i=&\frac{2\,(b-d)}{(b-c)^3}\left[(d-c)\,b_i'+(b-d)\,c_i'+(c-b)\,d_i'\right]\ln\left|\frac{V-b}{V-c}\right|\\&+\left[1-\left(\frac{b-d}{b-c}\right)^2\right]\ln\left|\frac{V-b}{V-c}\right|-\frac{b_i'}{V-b}\left(\frac{b-d}{b-c}\right)^2\\&-2\ln\left|\frac{V-d}{V-c}\right|-\frac{1}{V-c}\left(\frac{c-d}{b-c}\right)\\&\times\left[c-d+\frac{(c-d)\,b_i'+2\,(b-c)\,d_i'+2\,(c+d-2b)\,c_i'}{b-c}\right.\\&\left.-\frac{(c-d)\,c_i'}{V-c}\right].\end{aligned} \tag{23}$$

The special case of EOS with $k=0$ [or $c=d=0$] is identical to the repulsive part of the van der Waals EOS: $P=RT/(V-b)$. The fugacity coefficient can be given by a very simple form,

$$\ln\phi_i=-\frac{b_i'}{V-b} \tag{24}$$

The parameters b_i, c_i, and d_i ($k\neq 0$) for pure hard spheres (diameter of σ_i) have been determined so as to reproduce the actual hard-sphere properties at the solid–fluid phase equilibrium of Hoover and Ree [30]: $V_0/V_S=0.736\pm0.003$, $V_0/V_L=0.667\pm0.003$, $PV_0/RT=8.27\pm0.13$, where V_0 is the closest packing molar volume of hard spheres ($V_0=N_A\sigma_i^3/\sqrt{2}$), and the subcsripts S and L refer to solid and liquid phases, respectively. In the

case of EOS with k=1, $b_i = 1.32647V_0$, $c_i = 1.41055V_0$, and $d_i = 1.37252V_0$, while in the case of EOS with $k = 2$, $b_i = 1.32771V_0$, $c_i = 1.39782V_0$, and $d_i = 1.37850V_0$. The mathematical procedure for the parameter determination is given in Ref. 21.

3. ANALYSIS AND RESULTS

The phase-equilibrium condition is the equality of the chemical potential of each species among coexisting phases. In practice, the use of the fugacity coefficient is more convenient, and then the equilibrium condition for α, β, γ, ... phases is equivalently given by:

$$\phi_i^\alpha x_i^\alpha = \phi_i^\beta x_i^\beta = \phi_i^y x_i^y = \cdots \tag{25}$$

where $i = 1, \ldots, N$ ($N = 2$ for the present), and x is the composition in each phase at the same T and P. These equations are non-linearly coupled and often difficult to solve, particularly when the phase transition behavior is unknown in advance. For binary systems, the Gibbs free-energy plot at constant T and P is extremely useful to understand the phase behavior of unknown systems, since the so-called common tangent method can be used to construct the phase behavior characteristics. Furthermore, such a plot does not require any solution of coupled non-linear equations. The Gibbs energy function G is conveniently related to the fugacity coefficient and can be written in a dimensionless form,

$$\frac{G}{RT} = \sum_{i=1}^{2} x_i \ln \frac{\phi_i x_i}{\phi_i^0}, \tag{26}$$

where ϕ_i^0 is a pure component's fugacity coefficient at a system (T, P), and can be chosen at an arbitrary reference point.

It should be mentioned that T and P cannot be separate variables in the case of hard spheres and a T–P ratio becomes a thermodynamic variable. In the present study, we use a ratio RT/P as the variable, which has a molar volume unit but is normalized with the corresponding value $(RT/P)_{\mathrm{SL}}$ at the solid–liquid phase transition of the pure hard-sphere species (with a diameter σ_1),

$$(RT/P)_{\mathrm{SL}} = \frac{V_0}{Z_{\mathrm{SL}}} = \frac{N_{\mathrm{A}}\sigma_1^3}{\sqrt{2}Z_{\mathrm{SL}}}, \tag{27}$$

where the compressibility factor $Z_{\mathrm{SL}} = 8.27$ was taken from Ref. 30. Thus the normalized (dimensionless) RT/P is a relative volume, but also represents a relative temperature in an isobaric process or a relative inverse of

pressure in an isothermal process. In this work, the relative RT/P is called an effective temperature, τ (for an isobaric process).

The phase behavior characteristics of hard-sphere mixtures in the present model are controlled by the size ratio (γ), the effective "temperature" (τ, relative RT/P), and the binary interaction parameters (l_{ij}, m_{ij}, n_{ij}). In order to understand the phase behavior graphically, a computer program plotting Eq. (26) as a function of x has been made for any input of the control parameters. Using the computer program, we can visually inspect the phase equilibria of binary mixtures; the phase stability, metastability, and approximate compositions are instantly observed on a computer screen. This method has been extensively used in the present study. Once the phase behavior characteristics are known in this way, an actual phase diagram can be constructed by solving the non-linearly coupled equations Eq. (25), using a Newton–Raphson iteration method.

3.1. EOS with $k = 0$ [or $c = d = 0$]

Although the present purpose is to study systems with both solid and fluid phases, it is instructive to study a special case of Eq. (2) with $k=0$ (or $c=d=0$). It is simply the repulsive part of the van der Waals (fluid-only) EOS. The van der Waals EOS for mixtures is known to predict fluid–fluid separations (or de-mixing). Then the question arises whether only the purely repulsive part of the EOS in such a simple form can produce such a phase separation. This is an important and interesting question. The result may provide some insights for hard-sphere fluid phase transitions.

Since the fugacity coefficient is a simple form as given by Eq. (24), the Gibbs free energy can be written explicitly. A value of V in Eq. (24) is a solution of the EOS with $k=0$ at a given RT/P ratio, and is simply $V=RT/P+b$. b_i' in Eq. (24) can be written using Eq. (20) as

$$b_1' = -b_1 + l_{12}(b_1+b_2)x_2^2, \tag{28}$$

$$b_2' = -b_2 + l_{12}(b_1+b_2)x_1^2. \tag{29}$$

Then, the reduced Gibbs free energy, Eq. (26), becomes

$$\frac{G}{RT} = -\frac{P}{RT} l_{12}(b_1+b_2)x_1x_2 + x_1\ln x_1 + x_2\ln x_2, \tag{30}$$

where the reference point for each pure component was taken as $\ln\phi_i^0 = Pb_i/(RT)$, since the chemical potential of a pure component can be chosen arbitrarily. This result is very interesting, since it is the same form as

a well-known regular solution model [20, 25],

$$\frac{G}{RT} = \frac{z\varepsilon}{RT} x_1 x_2 + x_1 \ln x_1 + x_2 \ln x_2 \tag{31}$$

where z is an average coordination number of the nearest neighbors and $\varepsilon \equiv \varepsilon_{12} - (\varepsilon_{11} + \varepsilon_{22})/2$. ε_{ij} is the inter-particle potential energy of i–j nearest neighbor pairs, and can be purely repulsive (positive value) or purely attractive (negative value) with respect to the infinite separation of pairs. It is easy to show that if $\varepsilon > 0$, fluid–fluid separation (de-mixing) occurs, and the critical point of de-mixing is $z\varepsilon = 2RT_c$ It should be noted that the regular solution model contains the case of purely repulsive inter-particle potentials as well, and that the case of $\varepsilon \geq 0$ can occur for either purely repulsive or attractive ε_{ij}. From Eqs. (30) and (31), the following relationship holds:

$$\frac{z\varepsilon}{RT} = -\frac{P}{RT} l_{12} (b_1 + b_2) . \tag{32}$$

Therefore, in order for the present pure repulsive EOS to have any fluid de-mixing, the parameter l_{12} must be negative (for $\varepsilon > 0$), and then the critical condition is $\frac{P}{RT} l_{12} (b_1 + b_2) = -2$. A negative l_{12} means $\beta > 1$ (or $\alpha > 0$), and the fluid de-mixing occurs for the size ratioγ region satisfying a relation $(1-\gamma)^2 / \left(1 - \gamma + \gamma^2\right) < (\beta - 1)/3$; see Eq. (17).

Although the present repulsive EOS shows the possibility of fluid de-mixing, it is not certain whether such a phase separation can be thermodynamically stable with respect to the interference of solid–liquid phase equilibria. Furthermore, the present single-branch EOS may present a solid–state EOS instead of the liquid state, and the de-mixing may be an iso-structural solid–solid separation. Since the present EOS does not have both solid- and liquid-phase branches, this point must be studied with a solid–fluid EOS, which is the case of $k \neq 0$

3.2. EOS with $k = 1$

Using the computer program for the Gibbs-energy plot mentioned earlier, various phase behaviors have been found by changing the control parameters: the size ratio (γ), the effective temperature (τ, relative RT/P), and the binary interaction parameters (l_{ij}, m_{ij}, n_{ij}). Before analyzing the present EOS, we must know the proper magnitude of the interaction parameters. Although they are empirical and unknown parameters, they cannot be arbitrarily large and unbounded.

Let the parameter b_1 be the larger excluded volume and b_2 be the smaller one, without loss of generality. Then, a mixture's b with *any com-*

position must satisfy the following physical condition: $b_2 < b < b_1$. Using Eq. (4) and this relation (regardless of x), we arrive at

$$|l_{ij}| < \frac{b_1 - b_2}{b_1 + b_2} = \frac{2}{1+\gamma^3} - 1 < 1, \tag{33}$$

where $i \neq j$ and $0 < \gamma^3 \equiv b_2/b_1 < 1,$, defined in Eq. (15). It may be worth mentioning here that the condition in Eq. (33) restricts the validity range in the "non-additive" parameter β (or α) in Eq. (13) as well. Based on Eq. (17)

$$0 < \beta < 5, or -1 < \alpha < 5^{1/3} - 1 \approx 0.71. \tag{34}$$

For m_{ij} and n_{ij}, conditions similar to Eq. (33) should hold. In addition to Eq. (33), another constraint exists among the interaction parameters. The relationship that a parameter value in d is between b and c must be satisfied in order for the present EOS to be physically a correct form, as discussed in Ref. 21. This requirement can be analytically solved by applying the tangential condition to Eqs. (4)–(6). The allowed range of the interaction parameters depends upon the size parameter γ. At a given γ input to the Gibbs-energy plot program, the information of the allowed range is displayed on a computer screen, as well as the relative magnitude plot of the interaction parameters and simultaneously the Gibbs energy as a function of x. In this way, phase behavior characteristics of the present binary system are quickly examined visually using various proper input parameters.

After trial-and-error analysis of various combinations of input parameters, it has been found that the present EOS can simulate all basic phase-transition behaviors known for actual binary solid–liquid systems [20, 31], including rather unusual behaviors. This means that the solid–liquid equilibrium of actual substances is essentially governed by the repulsive (geometrical) factor. The size γ effect on phase behaviors is embedded in the interaction parameter. This may be understood by Eq. (17). The interaction parameter is a function of γ and β (or α), and the different size effect can be compensated with a proper set of interaction parameters. Generally, the larger the magnitude of the interaction parameter, the larger the size difference results, and *vice versa*. Therefore, in the following analysis we examine the general phase behavior in the case of a fixed value γ of 0.75, which can be regarded as an effective and general size difference. In the case of extreme differences such as $\gamma < 0.1$, the present mixing rule may not be applicable, and some discussion about very large size differences will be given in a later section.

Usually the phase diagram for binary mixtures is plotted as a temperature–composition ($T-x$) diagram at a constant pressure, or a

pressure–composition (P– x) diagram at a constant temperature. However, as mentioned earlier, in the case of hard-sphere mixtures T and P cannot be separated, and only the ratio (or the compressibility factor) is meaningful. In order to mimic the familiar T– x phase diagram, we use the "relative RT/P" defined in Section 3 as an effective "temperature" (τ) at constant pressure. Typical phase-behavior characteristics studied here are summarized in Figs. 1–7. They are plotted as τ–x (or "relative RT/P"–x) diagrams, where the size parameter γ is 0.75 for all cases and the interaction parameters l_{12}, m_{12}, and n_{12} are designated as l, m, and n, respectively.

Figures 1 and 2 show the case of l, m, and n with zero or positive values. Zero interaction parameter means the mixing is linear for b, c, or d (see Eqs. (4)–(6)), and then the non-additive parameter for $\gamma = 0.75$ becomes $\beta \approx 1.2308$ (or $\alpha \approx 0.07166$), based on Eq. (17). Figure 1a is such a case, and the system may be regarded as an ideal mixture. In the case of "additive" hard spheres ($\beta = 1$, or $\alpha = 0$), the interaction parameter l, m, or n becomes about 0.05769, as shown in Fig. 1b, which is nearly ideal. Further increases in l, m, and n values do not change the topology of the phase diagram. However, when a part (one or two) of the three interaction parameters is non-linear (quadratic) and the other is linear, the phase behavior can become highly non-ideal, as shown in Figs. 1c, d, and 2a–d. Maximum and minimum azeotropies (Figs. 1c, d, 2a, and c) appear. The former cases do not have solid–solid separations, while the latter cases show iso-structural solid–solid phase separation at a low relative RT/P. Figure 2b, d show rather unusual and complicated phase diagrams. Figure 2b possesses two peritectic points, a minimum azeotropy, and a eutectoid, while Fig. 2d has two eutectic points, a maximum azeotropy, and two miscibility gaps with lower critical solution temperatures (LCST) in the solid state.

Figures 3–7 show an analysis in the case of zero and negative interaction parameters, where all cases have the solid–solid phase separation. In Fig. 3, several familiar phase diagrams are simulated: spindle-like (near ideal) liquidus–solidus lines, a minimum azeotropy with a solid–solid miscibility gap at low RT/P, and a simple eutectic point. In Fig. 4, the effect of the interaction parameter l with $m = n = 0$ is examined. The decrease in l produces progressively complex phase diagrams: minimum azeotropy, "upper critical solution temperature" (UCST) in the solid and a monotectic point (Fig. 4a); eutectic, UCST, and monotectic (Fig. 4b); eutectic, peritectic, and monotectic (Fig. 4c); two eutectic, maximum azeotropy, and eutectoid (Fig. 4d). Figure 5 shows the effect of values for $l = m = n$, which are continuations of the case of Fig. 3a. With a sufficiently large value of the interaction parameter (Fig. 5b), a liquid–liquid

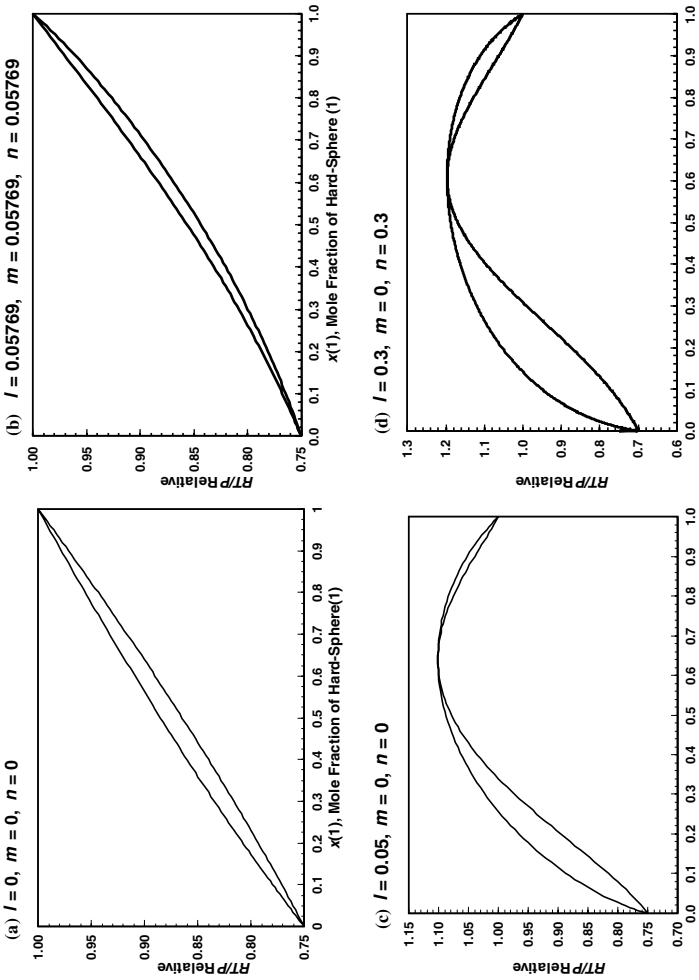

Fig. 1. Phase diagrams of binary hard-sphere (1)/(2) mixtures: relative RT/P vs. mole fraction. The relative RT/P is a normalized molar volume but also represents an effective temperature for an isobaric process. The size ratio of the binary hard spheres is 0.75. The parameters l, m, and n are the adjustable binary parameters in the quadratic mixing rule, and are written as l_{ij}, m_{ij}, and n_{ij} in the text, respectively.

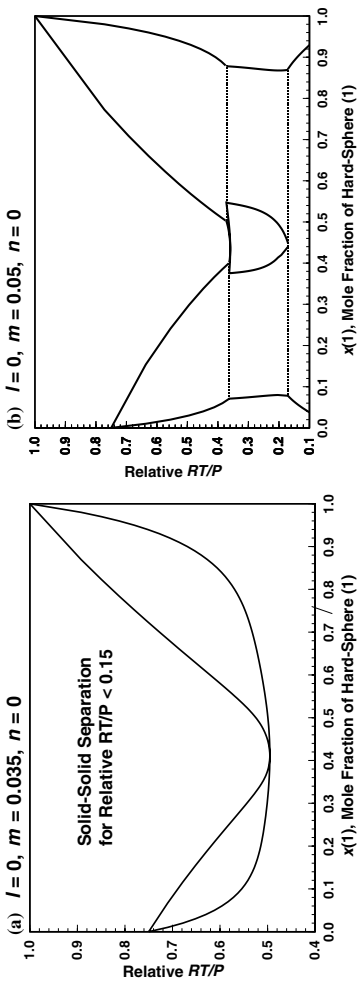

Fig. 2. Phase diagrams of binary hard-sphere (1)/(2) mixtures: relative RT/P vs. mole fraction. See more details in the figure caption of Fig. 1. The horizontal dotted lines are the triple-point lines.

separation (de-mixing) occurs, and the phase diagram has an UCST and two peritectic points. The increase in l from -0.125 to -0.135 while keeping the same $m=-0.100$ and $n=-0.135$ produces also a liquid–liquid separation with an UCST but two eutectic points (Fig. 6). Figure 7 shows a subtle effect of n while keeping $l=m=-0.125$; one of the peritectic points in Fig. 7a becomes a eutectic point with an increase in the n value (Fig 7b).

3.3. EOS with $k = 2$

As mentioned in Ref. 21, the phase-behavior characteristics of EOS with a general k value are expected to be at least qualitatively the same as those in EOS with $k=1$, although a higher- k EOS would improve the volumetric properties. In fact, the well-known solid–fluid phase transition of identical hard spheres was equally well reproduced using EOS with $k=2$. Then only b,c, and d parameters must be changed and are somewhat different from those in EOS with $k=1$: refer to the end of Section 2. In order to investigate whether any new phase behavior occurs in hard-sphere mixtures with a different EOS, the phase behavior using EOS with $k=2$ has been investigated. The analysis has been easily made using the Gibbs-energy plot program mentioned earlier, since the computer program is made so as to be able to switch EOS between $k=1$ and $k=2$ on the same IO (input/output) screen. Thus, two EOS results are quickly examined and compared. As expected, EOS with $k=2$ produced the same topological phase behaviors as those in EOS with $k=1$. The same topology of the phase characteristics was made simply using a set of interaction parameters somewhat different from those in EOS with $k=1$.

4. DISCUSSION

The present analytical EOS for hard-sphere mixtures seems useful for understanding the topology of the solid–liquid phase transition characteristics of binary hard-sphere mixtures. Although they are by no means exhausted, the types of phase diagrams produced are surprisingly rich, and the present results will provide some useful insights on theoretical studies of binary hard spheres. In addition, the results show good qualitative descriptions for the phase-transition behavior of actual substances [20, 31]. For example, the rather complicated and curious shape of the phase diagram predicted in Fig. 4b represents an excellent topology for actually observed binary alloys (Al-Zn system) [20, 32], as compared in Fig. 8. Other complex shapes of phase diagrams shown in Figs. 2b, 2d, and 4d are actually illustrated in a textbook [31], except for the LCST predicted

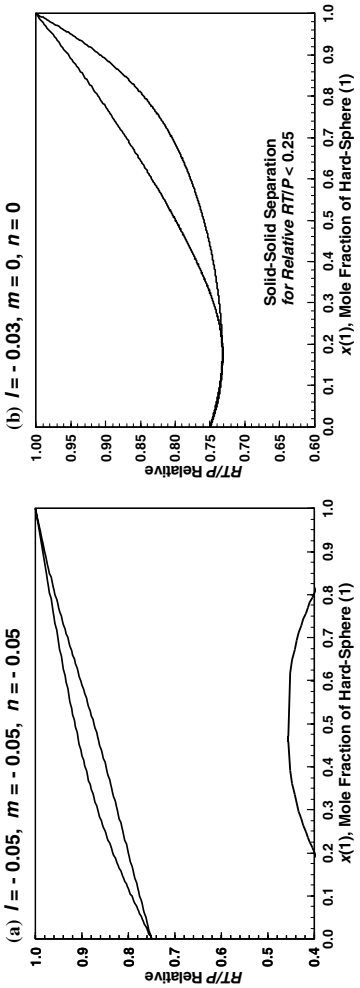

Fig. 3. Phase diagrams of binary hard-sphere mixtures: relative RT/P vs. mole fraction. See more details in the figure caption of Fig. 1. The horizontal dotted lines are the triple-point lines.

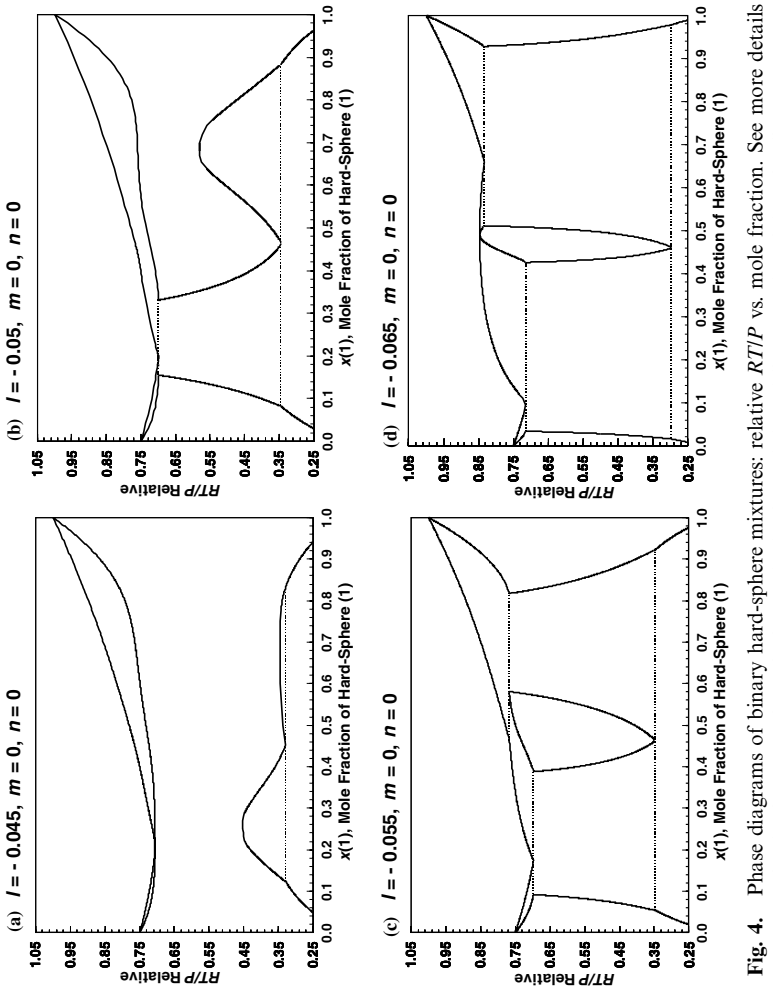

Fig. 4. Phase diagrams of binary hard-sphere mixtures: relative RT/P vs. mole fraction. See more details in the figure caption of Fig. 1. The horizontal dotted lines are the triple-point lines.

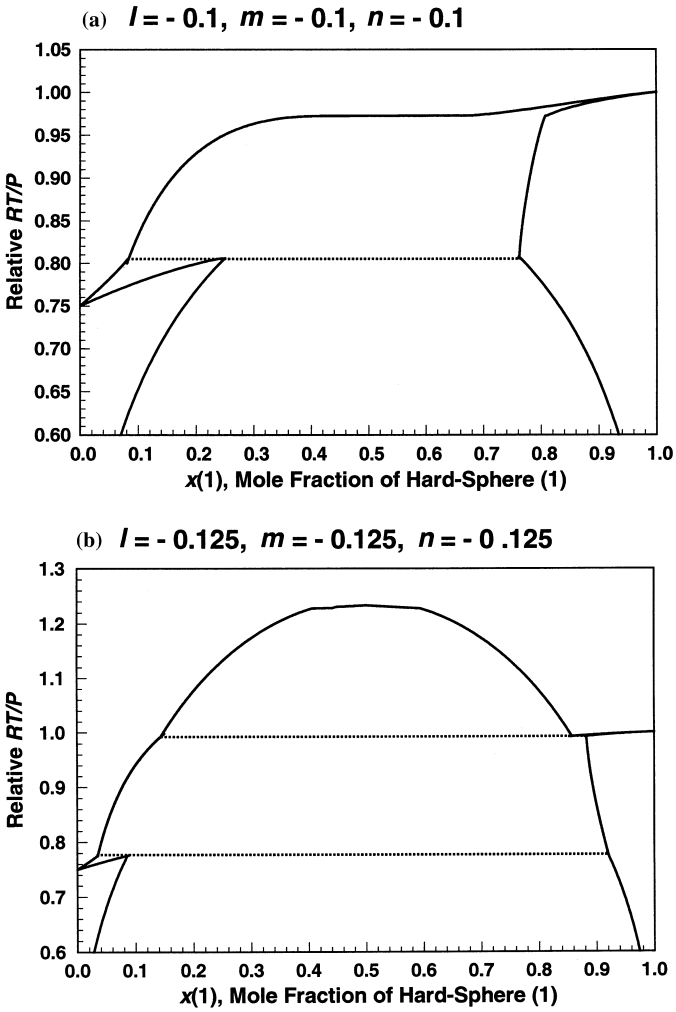

Fig. 5. Phase diagrams of binary hard-sphere mixtures: relative RT/P vs. mole fraction. See more details in the figure caption of Fig. 1. The horizontal dotted lines are the triple-point lines.

in the solid solution of Fig. 2d, which seems to be a newly discovered feature, although such behaviors are quite common in liquid solutions [28].

The validity of the present mixing model should be discussed here. As mentioned in Section 3, the quadratic mixing (or random mixing) model is incorrect in the case of a large size difference and a high density. However,

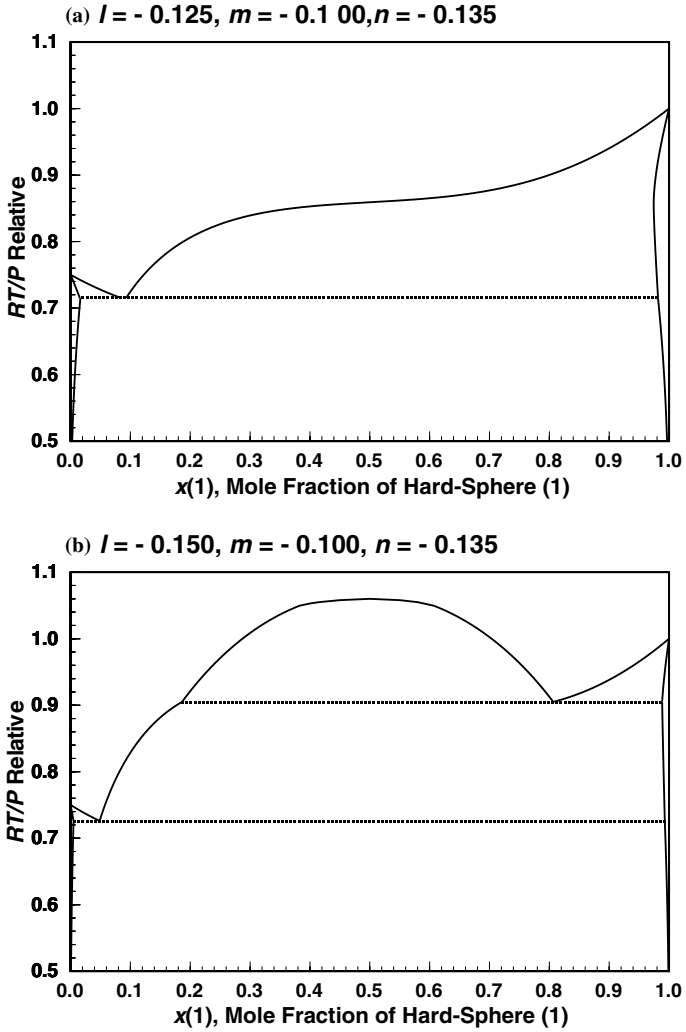

Fig. 6. Phase diagrams of binary hard-sphere mixtures: relative RT/P vs. mole fraction. See more details in the figure caption of Fig. 1. The horizontal dotted lines are the triple-point lines.

with the use of effective interaction parameters (l_{12}, m_{12}, n_{12}), the qualitative features of phase diagrams appear to be correct for all size ratios, although we did not investigate extreme cases ($\gamma \ll 1$). Such extreme cases are surely beyond the validity of the present model. The valid size ratio for the present model may be $\gamma > 0.1547$, which is the case when a smaller

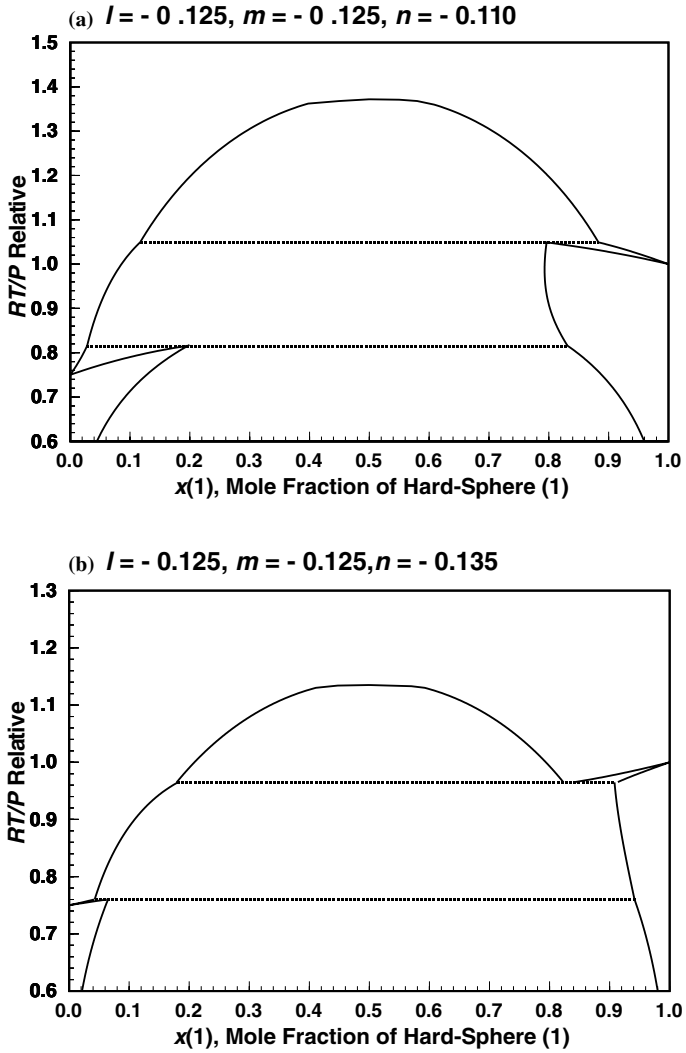

Fig. 7. Phase diagrams of binary hard-sphere mixtures: relative *RT*/*P* vs. mole fraction. See more details in the figure caption of Fig. 1. The horizontal dotted lines are the triple-point lines.

sphere can be just accommodated within the holes of the array formed by mutually touching larger spheres:$\gamma = 2/\sqrt{3} - 1 \approx 0.1547$. When $\gamma \ll 0.1547$, qualitatively different behaviors for the solid–liquid phase transitions may occur, since small spheres can act like pure hard spheres inside the interstices of large spheres (or large spheres act like simple walls of a

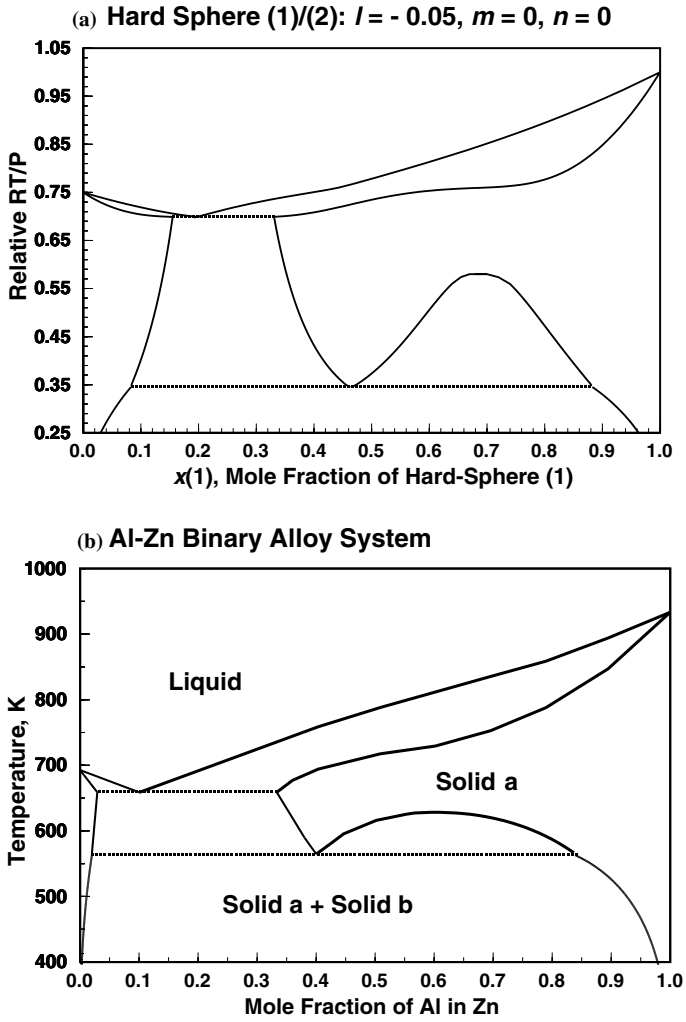

Fig. 8. Phase diagrams of binary hard-sphere (1)/(2) mixtures: relative RT/P vs. mole fraction (the same as Fig. 4b). (b) Observed T–x phase diagram of aluminum–zinc binary alloys [20, 32]. The horizontal dotted lines are the triple-point lines.

container). In order to study such extreme asymmetric size mixtures, the empirical mixing parameters (l_{12}, m_{12}, n_{12}) must be treated as a function of mole fraction, instead of the effective average constant for the random mixing model.

In the present study on solid–liquid phase behavior, we have examined two types of EOS with $k=1$ and $k=2$. The qualitative phase behaviors with both EOS are the same. A higher k value EOS will also give similar results, although the higher k EOS would improve the numerical accuracy of volumetric properties [21]. The use of a simpler low- k EOS to analyze phase behavior may be justified by the known fact of usual vapor–liquid phase equilibria: the TPx (temperature–pressure–composition) diagram is not very sensitive to the volumetric properties. For example, a simple cubic EOS can accurately describe observed vapor–liquid TPx diagrams, although the liquid density in such an EOS is poorly predicted.

As mentioned in Section. 2, another type of EOS for hard spheres can be considered based on the idea of the statistical (kinetic) attraction in the purely repulsive interaction of a high-density system. Then, a general form can be written as $P/RT = (\text{repulsive term}) - (\text{“kinetic” attraction term})$, where both terms are T independent. In fact, an analytically closed hard-sphere EOS [33] which reproduces well both solid and liquid branches of the Monte Carlo computer simulations of hard spheres has exactly this type of form, although the EOS required a large number of constants, as many as 18 constants. An empirical EOS form with an extra attractive term for the solid–liquid–vapor state by Wenzel and Schmidt [34] can be justified by the present interpretation (“kinetic attraction” term), except for the T dependence of the added attractive term, which results in an existence of a critical point in the solid–liquid phase equilibrium. One of the simplest such forms will be $P/RT = 1/(V-b) - d/(V-c)^2$, which can possess a solid–liquid phase transition with proper positive b, c, d constants with a condition of $b > c$. This type of EOS was also examined in the present study with the same mixing rule for the EOS constants, and then, we have found qualitative phase behaviors similar to those in the present EOS.

The present result revealed rich solid–liquid phase diagrams, and adding the vapor phase contribution will be made without much difficulty using Eq. (1) with the attractive term. Then we can study the global topological classification of vapor–liquid–solid phase behaviors of binary mixtures. The present study is the starting point for such a study. Lamm and Hall [19] have attempted such a classification for the Lennard-Jones potential fluid using Monte Carlo computer simulations. However, some interesting topologies in solid–solid phase behavior at low temperatures (see Figs. 2 and 4) have not been studied, and critical point phenomena cannot be evaluated in their method, although they claimed that “the complete phase diagram was constructed.” In addition, it is worth mentioning that the computational burden to construct the phase diagram is minimum with the present simple analytical EOS, even in the case

of highly complex diagrams such as Fig. 4c, d, which require six and seven separate phase-equilibrium calculations for solid–liquid and solid–solid phases. Each phase-equilibrium calculation needs less than 1 or 2 s with modern PC computers, compared with many hours for Monte Carlo computations.

5. CONCLUSIONS

We have demonstrated that the present simple analytical EOS can simulate various basic topological features of solid–liquid phase equilibria of binary hard spheres, including highly complex phase diagrams with the combination of basic diagrams. Although the present catalog of phase diagrams for binary mixtures is by no means exhaustive, it has already shown some new features. Complex behaviors of the interplay in solid–liquid and liquid–liquid phase transitions can be observed by systematically changing the binary interaction parameters.

The empirically introduced interaction parameters may be justified as an effective average correction for the quadratic (random) mixing rule, and as far as the qualitative prediction of phase behavior is concerned, the present quadratic mixing seems reasonable. The interaction parameters are closely related to the size difference of hard spheres, and thus their physical meanings can be understood as the size-difference effect.

The present study is a starting point and highly useful for constructing the complex global topological classification of solid–liquid–vapor phase diagrams of binary mixtures.

REFERENCES

1. M. Dijkstra, R. van Roij, and R. Evans, *Phys. Rev. E* **59**: 5744 (1999).
2. C. A. Croxton, *Introduction to Liquid State Physics* (John Wiley, London, 1975).
3. M. S. Wertheim, *Phys. Rev. Lett.* **10**: 321 (1963); E. Thiele, *J. Chem. Phys.* **38**: 1959 (1963); Thiele, *J. Chem. Phys*. **39**: 474 (1963).
4. J. G. Kirkwood and E. M. Boggs, *J. Chem. Phys.* **10**: 394 (1942).
5. B. J. Alder and T. E. Wainwright, *J. Chem. Phys.* **27**: 1208 (1957); B. J. Alder and T. E. Wainwright, *J. Chem. Phys*. **33**: 1439 (1960).
6. W. W. Wood and J. D. Jacobson, *J. Chem. Phys.* **27**: 1207 (1957).
7. C. A. Croxton, *J. Phys.* C **7**: 3723 (1974) .
8. A. Yu. Valasov and A. J. Masters, *Proc. 16th European Conf. Thermophysical Properties*, September 1–4 (2002), London, United Kingdom.
9. R. Roth, R. Evans, and A. A. Louis, *Phys. Rev* . E **64**: 051202 (2001).
10. M. Dijkstra, R. van Roji, and R. Evans, *Phys. Rev. Lett.* **81**: 2268 (1998).
11. R. Roth, R. Evans, and S. Dietich, *Phys. Rev* . E **62**: 5360 (2000).
12. R. Roth and R. Evans, *Europhys. Lett.* **53**: 271 (2001).
13. R. Roth, R. Evans, A. Lang, and G. Kahl, *J. Phys.: Condens. Matter* **14**: 12063 (2002).

14. J. Largo, M. J. Maeso, and J. R. Solana, *Proc. 16th European Conf. Thermophysical Properties*, September 1–4 (2002), London, United Kingdom.
15. M. K. Khoshkarchi and J. H. Vera, *Fluid Phase Equilibr.* **142**: 131 (1998).
16. M. Schmidt, H. Loewen, J. M. Brader, and R. Evans, *J. Phys.: Condens. Matter* **14**: 9353 (2002).
17. J. Vieillard-Baron, *J. Chem. Phys.* **56**: 4729 (1972).
18. D. A. Kofke, *J. Chem. Phys.* **98**: 4149 (1993); D. A. Kofke, *Adv. Chem. Phys.* **105**: 405 (1999).
19. M. H. Lamm and C. K. Hall, *AICHE J.* **47**: 1664 (2001).
20. C. H. P. Lupis, *Chemical Thermodynamics of Materials* (North-Holland, New York, 1983).
21. A. Yokozeki, *Int. J. Thermophys.* **24**: 589 (2003).
22. D. C. Garcia and K. D. Luks, *Fluid Phase Equilibr.* **161**: 91 (1999).
23. J. A. Labadie, D. C. Garcia, and K. D. Luks, *Fluid Phase Equilibr.* **171**: 11 (2000).
24. P. H. Konynenberg and R. L. Scott, *Philos. Trans. R. Soc. Lond.*, *Ser.* A **298**: 495 (1980).
25. J. H. Hildebrand, J. M. Prausnitz, and R. L. Scott, *Regular and Related Solutions* (Van Nostrand Reinhold, New York, 1970).
26. J. E. Mayer, *J. Phys. Chem.* **43**: 71 (1939).
27. A. Yokozeki, *Int. J. Thermophys.* **22**: 1057 (2001).
28. J. S. Rowlinson and F. L. Swinton, *Liquid and Liquid Mixtures* (Butterworths, London, 1982).
29. H. C. Van Ness and M. M. Abbott, *Classical Thermodynamics of Nonelectrolyte Solutions* (McGraw-Hill, New York, 1982).
30. W. G. Hoover and F. H. Ree, *J. Chem. Phys.* **49**: 3609 (1968).
31. S. M. Walas, *Phase Equilibria in Chemical Engineering* (Butterworths, Boston, 1985), pp. 265–277.
32. R. Hultgren, P. D. Desai, D. T. Hawkins, M. Gleiser, and K. K. Kelly, *Selected Values of the Thermodynamic Properties of Binary Alloys* (Am. Soc. Metals, Metals Park, OH, 1973).
33. J. G. Loeser, Z. Zhen, S. Kais, and D. R. Herschback, *J. Chem. Phys.* **95**: 4512 (1991).
34. H. Wenzel and G. Schmidt, *Fluid Phase Equilibr.* **5**: 3 (1980).